



Cite this: *Biomater. Sci.*, 2018, **6**, 2298

Received 8th May 2018,  
Accepted 18th July 2018  
DOI: 10.1039/c8bm00516h  
rsc.li/biomaterials-science

## Boron nitride nanomaterials: biocompatibility and bio-applications

A. Merlo,<sup>a</sup> V. R. S. S. Mokkalpati,<sup>b</sup> S. Pandit<sup>b</sup> and I. Mijakovic<sup>\*b</sup>

Boron nitride has structural characteristics similar to carbon 2D materials (graphene and its derivatives) and its layered structure has been exploited to form different nanostructures such as nanohorns, nanotubes, nanoparticles and nanosheets. Unlike graphene and other carbon based 2D materials, boron nitride has a higher chemical stability. Owing to these properties, boron nitride has been used in different applications as a filler, lubricant and as a protective coating. Boron nitride has also been applied in the biomedical field to some extent, but far less than other 2D carbon materials. This review explores the potential of boron nitride for biomedical applications where the focus is on boron nitride biocompatibility *in vivo* and *in vitro*, its applicability as a coating material/composite and its anti-bacterial properties. Geometry, material processing and the type of biological analysis appear to be relevant parameters in assessing boron nitride bio-compatibility. Engineering of both these variables and the coating would open the door for some applications in the medical field for boron nitride, such as drug delivery, imaging and cell stimulation.

<sup>a</sup>Department of Applied Science and Technology, Politecnico di Torino, Corso Duca degli Abruzzi 24, Torino 10129, Italy

<sup>b</sup>Systems and Synthetic Biology, Department of Biology and Biological Engineering, Chalmers University of Technology, Kemivagen 10, Goteborg 41329, Sweden.  
E-mail: ivan.mijakovic@chalmers.se

### Introduction

Boron nitride (BN) is a refractory material made of boron and nitrogen. It can crystallize in different forms depending on pressure and temperature<sup>1,2</sup> (hexagonal, rhomboedral, diamond-like cubic<sup>3</sup> and wurzite<sup>4</sup>), but its most stable form at room temperature is the hexagonal form. This configuration is



Alessandra Merlo

Alessandra Merlo received her Master's degree in Materials Science and Engineering from Politecnico di Torino, Italy (2018). After an exchange period at Iowa State University, she conducted her Master's thesis work at Chalmers University of Technology, Goteborg, Sweden, in bio-medical applications of graphene-based biosensors. Her research interest ranges from medical applications of materials to archeological and textile materials.



V. R. S. S. Mokkalpati

V. R. S. S. Mokkalpati acquired his Ph.D. from Delft University of Technology, The Netherlands, in 2011. Prior to starting his career as a Researcher at Chalmers University of Technology, he worked as a Research Fellow at Austrian Institute of Technology, National University of Singapore and Sabanci University. His areas of expertise include design, fabrication and testing of Micro/Nano fluidics in bio-medical applications, 2D/3D Graphene based sensors, Medical diagnostics, Lab-on-a-chip devices, Bioengineering, Graphene/graphene derivative-based ultrafiltration membranes and Graphene window for TEM studies. He is a recipient of FP-7 Marie-Curie co-fund fellowship for his work related to graphene integrated membranes for ultrafiltration of body fluids.



characterized by the disposition in layers of hexagons of alternating boron and nitrogen atoms, similar to graphene structure. The hexagonal layer plane features strong covalent bonds with a spacing almost identical to that in graphene. The layers forming the three-dimensional structure are kept together through van der Waals forces, as B and N atoms align alternately in a vertical direction, as described in ref. 5. Owing to structural characteristics very similar to graphene, this material attracted increasing attention in recent years, as its layered structure was exploited to form different nanostructures such as boron nitride nanotubes, nanosheets, nanohorns and nanoparticles with different shapes.<sup>4</sup>

While structurally very similar to its carbon counterpart, BN is characterized by specific and unique properties which represent a considerable advantage in some specific applications. Unlike graphene, whose band gap depends on chirality and diameter, BN has a consistent gap of 5.5–6 eV<sup>6,7</sup> when reduced from bulk to layer form. Unique mechanical properties<sup>8–11</sup> and thermal conductivity,<sup>12,13</sup> combined with a remarkable anti-oxidation capacity<sup>14</sup> of BN could be exploited to enhance properties of various composites. While the addition of carbon nanostructures to polymers may compromise the electrical insulation, in the case of BN the dielectric properties would be retained. Compared to its carbon-based counterparts which are colored (mostly black), BN is white colored and would allow dyeing, which might be of interest in the medical field. Its optical properties are applicable in the UV-regime, which distinguishes it from carbon nanotubes that absorb in the IR range. Finally, BN was found to possess remarkable piezoelectric properties,<sup>15</sup> a feature that opened up new scenarios for innovative applications.

BN is chemically more stable than carbon nanomaterials and so to improve the dispersibility in aqueous solutions, surfactants are often used.<sup>16</sup> Surfactants are rather used in two

different ways in the case of BN: (1) as co-solvents during exfoliation<sup>17,18</sup> of BN nanosheets and (2) for direct dispersion.<sup>19</sup> Given these distinctive dispersion parameters, BN has thus far been used in many different fields for different goals: as a filler in composites to improve both mechanical<sup>20</sup> and thermal properties, as a lubricant<sup>21</sup> for protective coatings<sup>22–25</sup> in cosmetic products,<sup>26</sup> and also for hydrogen storage.<sup>27,28</sup>

Considering the analogy with the carbon structures to which BN is very similar, this material has attracted a considerable interest in the biomedical field in the recent years. Nevertheless, its use in biomedical applications is still lagging behind that of carbon structures.

Employment of carbon nanostructures, especially carbon nanotubes, has been investigated in biosensing, imaging and cancer cell targeting, but the debated degree of cytotoxicity of these carbon nanomaterials<sup>29–31</sup> has opened up venues for developing alternative, non-toxic solutions and materials. In fact, while functionalization may limit the cytotoxicity of the material, the possibility of *in situ* desorption does not completely eliminate the toxic effects. The superior chemical inertness of BN with respect to carbon nanostructures constitutes a strong argument for using this material as a replacement of carbon nanostructures in biomedical applications.

### Biocompatibility *in vitro*

In 2008, Chen *et al.* reported compatibility of BN nanotubes with kidney cells.<sup>32</sup> These nanotubes are tubular with a structure analogous to that of carbon nanotubes. The multi-walled BN nanotubes in this study were produced through CVD (Chemical Vapor Deposition) process<sup>33</sup> to obtain final lengths of up to 10  $\mu\text{m}$ , and outer diameters around 20 nm (Fig. 1). These nanotubes, without any functionalization (concentration of 100  $\text{mg mL}^{-1}$ ) were tested on kidney cells and shown to not exhibit any cytotoxicity. Further, these nanotubes were coated



**Santosh Pandit**

*Santosh Pandit is a Post-doctoral researcher at the department of Biology and Biological Engineering, Chalmers University of Technology, Sweden. He obtained his Ph.D. degree from Chonbuk National University, Republic of Korea. His current research focuses on the antimicrobial coatings of graphene and other 2D materials on biomedical devices to prevent the device associated infections. His research also focuses on the*

*development of antimicrobial/anti-biofilm agents to prevent the biofilm associated infection as well as to reduce the possibility of antimicrobial resistance development.*



**Ivan Mijakovic**

*Ivan Mijakovic is a Chaired Professor of Bacterial Systems Biology and Director of the Area of Advance Life Science Engineering at the Chalmers University of Technology, Sweden. He is also Professor and group leader at the Technical University of Denmark. Prof. Mijakovic obtained his Ph.D. degree from the University Paris XI. He is an expert on bacterial protein phosphorylation and signaling, and his group investi-*

*gates the physiology of bacterial model organisms and pathogens. The Mijakovic group also develops metabolic engineering strategies, and new approaches to fight bacterial infections: novel anti-bacterial agents, coatings, and graphene-based sensors for infection.*



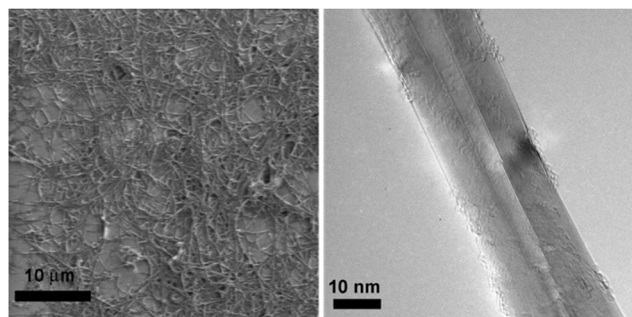


**Fig. 1** Structural characterization of pristine multiwalled BNNTs with high purity and high quality. (a) The SEM image of BNNTs. (b) High resolution TEM image of a BNNT. Reproduced with permission from *J. Am. Chem. Soc.*, 2009, **131**, 890–891. Copyright 2008 ACS.<sup>32</sup>

with glycodendrimer, which was engineered in order to bind specifically to the cell surface. The coated BNNTs were also not toxic.<sup>34</sup> As stated above, without any functionalization these nanotubes are likely to aggregate, and that would necessarily impact the results of compatibility assays. If the same kidney cells were to be probed with non-aggregated nanotubes, given the shape, aspect ratio and active surface, the results might vary. Therefore, further studies are needed to assess the biocompatibility of non-aggregated BNNTs.

Horváth *et al.* reported the cytotoxicity of BNNTs and proved that the toxicity is a function of both time of exposure and concentration.<sup>36</sup> In this study, multi-walled BNNTs, with an average length of 10 μm were produced by CVD, followed by secondary treatments such as high temperature annealing in Ar and acid washing. The nanotubes in solution, de-aggregated thanks to the use of a biocompatible surfactant, were then tested on human lung adenocarcinoma epithelial cells, human embryonic kidney cells, murine embryonic fibroblast cells and murine alveolar macrophage cells in different concentrations. Toxic effects were visible already after 48 h compared to controls, with a marked dependence not only on the time of exposure and concentration, but also on the cell line examined. Higher concentration and time of exposure led to lower cell viability, combined with a change in morphology and metabolism (Fig. 2).

In accord with previous results obtained on CNTs,<sup>37</sup> toxic effects were most severe for macrophage cells, while the kidney cells were most resistant. This suggested that cytotoxicity might be related to the predisposition to phagocytosis of the tested cells, *i.e.* their natural capacity to internalize nanotubes. The reported cytotoxicity of BNNTs towards kidney cells<sup>31</sup> was much higher compared to the BNNTs toxicity reported in a previous report on the same kind of cells.<sup>32</sup>

The study of Horváth *et al.*<sup>36</sup> emphasized the necessity of ulterior research on the biocompatibility of boron nitride nanostructures, pointing out that different factors affect their interaction with cells.

Ciofani *et al.*<sup>38</sup> conducted cytotoxicity tests on multi-walled BNNTs produced with the same method used by Horváth *et al.*,<sup>36</sup> but shortened to an average length of 1.5 μm. The

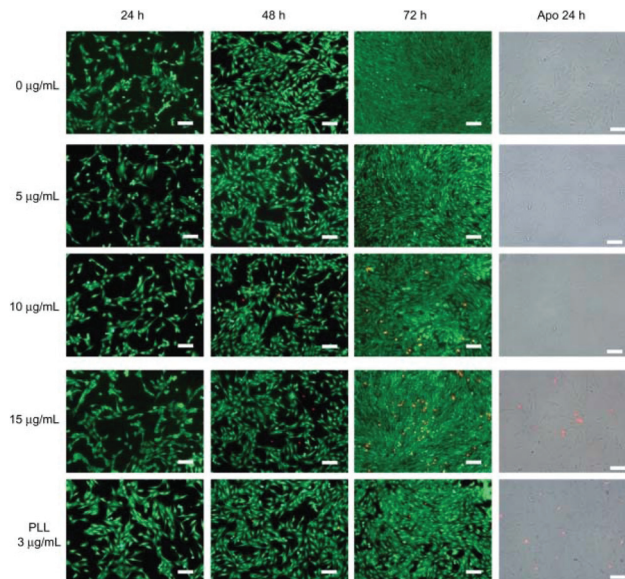


**Fig. 2** LIVE/DEAD® viability/cytotoxicity assay and early apoptotic detection (annexin V-FITC/PI assay) performed for different incubation times and concentrations. Note: Scale bar: 100 μm. Reproduced with permission from *Int. J. Nanomed.*, 2010, **5**, 285–298. Copyright 2010 Dove press.<sup>35</sup>

length difference led to very different results on bio-compatibility. In this case, gum arabic was used to disperse and stabilize the nanotubes suspension, which was tested on neuroblastoma cells and human umbilical vein epithelial cells with progressively increasing concentrations from 0 to 100 μg mL<sup>-1</sup>, for up to 72 h. While doses of 50 and 100 μg mL<sup>-1</sup> proved to be toxic towards both kind of cells; concentrations of up to 20 μg mL<sup>-1</sup> did not indicate any adverse effect on cell metabolism or in cell morphology after 24 h. No change of neuroblastoma cells differentiation was observed (Fig. 3).

Fluorescence analysis for detection of reactive oxygen species in the epithelial line showed no relevant sign of oxidative stress up until 48 h. TEM observations on epithelial cells established that the morphology and shape of the nanotubes, once phagocytised, did not change. Their spatial orientation when internalized was random, and they were always in the cytoplasm, never in the nuclei. According to these observations, the display of cytotoxicity in previous reports<sup>36</sup> may have been influenced by the dimensions of the nanotubes used, in line with some previous observations on carbon nanotubes toxicity on cells.<sup>39</sup>

In an attempt to evaluate the toxicity of BN on cells, Ciofani *et al.* came to an interesting result concerning cell viability measured through MTT (3-(4,5-dimethylthiazol-2-yl)-2,5-diphenyltetrazolium bromide) assays<sup>40</sup> that are extensively used to evaluate biocompatibility. In this study, BNNTs were obtained through a self-propagation, high-temperature synthesis process.<sup>41</sup> After 48 hours of incubation with human neuroblastoma cells, the MTT assay revealed a significant MTT decrement for concentrations around 20 μg mL<sup>-1</sup>. This finding



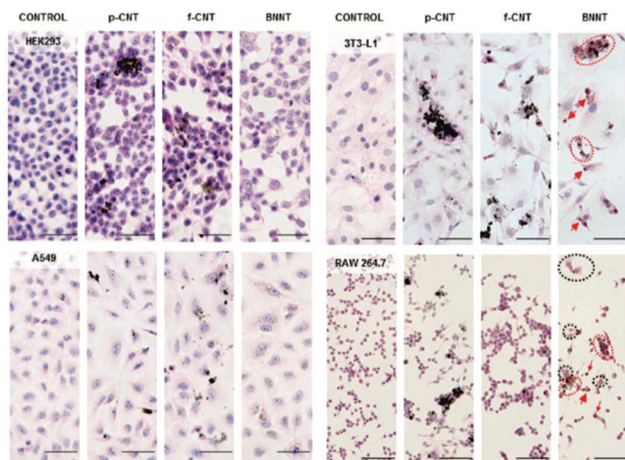


**Fig. 3** Cytopathological analyses of HEK293 kidney cells (first row), A549 epithelial cells (second row), 3 T3-L1 fibro-blasts (third row), and RAW 264.7 macrophages (fourth row) not treated with ENMs (control, first column) and treated for 4 days with approximately  $2 \mu\text{g mL}^{-1}$  of p-CNT (second column), f-CNT (third column), and BNNT (fourth column). BNNT-treated RAW 264.7 and 3 T3-L1 cells revealed characteristic alterations in morphology. These included disrupted cell to cell contacts leading to a more rounded appearance, due to cell retraction (eosinophilia). Consequently, the cytoplasmic staining was stronger (red circles), and cells with picnotic nuclei were present (red arrows). In addition, large multinucleated cells (black circles) undergoing frustrated phagocytosis were observed in the RAW 264.7 macrophages. Scale bars are  $50 \mu\text{m}$ . Reproduced with permission from *ACS Nano*, 2011, 5, 3800–3810. Copyright 2011 ACS.<sup>36</sup>

was in contrast to microscopic observations of different cell cultures treated in the same way for the same amount of time. Both treated and untreated cells did not show any significant difference in cellular density or morphology. The use of different assays allowed to highlight an interference with the MTT assay, especially for high concentrations of boron nitride particles, that resulted in false results about elevated cytotoxicity. In fact, as observed under the microscope, cell viability decreased with respect to controls only at concentrations superior to  $50 \mu\text{g mL}^{-1}$ , and cell proliferation was non-impacted. In turn, this proved that even at concentrations as high as  $100 \mu\text{g mL}^{-1}$ , boron nitride particles would still be biocompatible, and the toxicity results obtained with the MTT assay are to be interpreted with caution (Fig. 4 and 5).

Mateti *et al.*<sup>42</sup> reported another interesting observation on the biocompatibility of boron nitride nanosheets. They produced nanoparticles in different dimensions through a process of ball milling in argon, and ammonia for nanosheets in order to allow the exfoliation of sheets.<sup>43</sup> The time spent in the mill and the dimension of the final product were inversely proportional (the precursor powders used for the milling process had a dimension of  $15 \mu\text{m}$  for around  $2 \mu\text{m}$  in thickness). The process delivered nanoparticles with a spherical shape and a diameter range of 100 to 200 nm. Two major sub-groups of nanosheets were identified, one with an average diameter of  $1 \mu\text{m}$  for 100 nm in thickness, while the second group had a diameter of around 100 nm and 3 nm in thick-

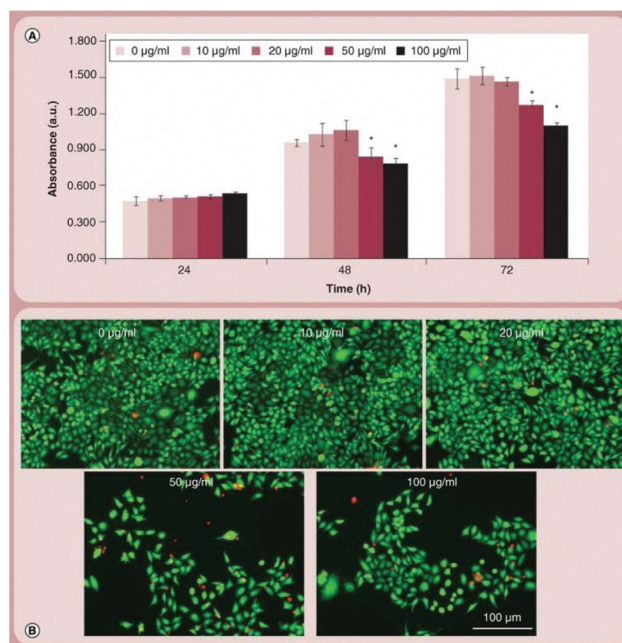


**Fig. 4** Cytopathological evaluation on SH-SY5Y cells. (A) WST-1 assay results on cultures treated with  $0$ – $100 \mu\text{g mL}^{-1}$  of BNNTs for 24, 48 and 72 h; (B) Live/Dead® staining performed after 72 h of treatment. Reproduced with permission from *Nanomedicine*, 2014, 9, 773–788. Copyright 2014 Future Medicine.<sup>38</sup>

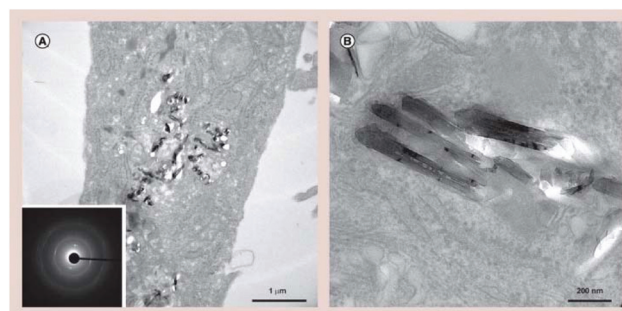


**Fig. 5** Boron nitride nanotube uptake investigation. (A) Low- and (B) high-magnification transmission electron microscopy images of boron nitride nanotubes internalized by human umbilical vein endothelial cells. Electron diffraction analysis of boron nitride nanotubes showed in the inset of (A). Reproduced with permission from *Nanomedicine*, 2014, 9, 773–788. Copyright 2014 Future Medicine.<sup>38</sup>

ness. The tests on cell viability of human osteosarcoma cells conducted in the presence of the material in its different shapes and forms indicated a progressive decrease in biocompatibility with the decrement of the size of both the particles and nanosheets.

The cell viability tests were backed up by light microscopy images. From the analysis of elemental composition of the cellular culture media used to test the toxicity of increasing concentrations of material, it was evident that there was significant change in boron content (Fig. 6 and 7).



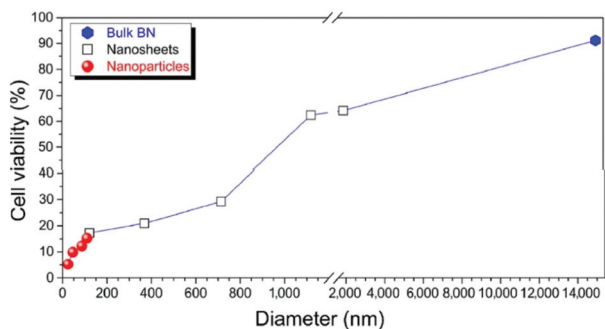


**Fig. 6** Percentage cell viability of SaOS<sub>2</sub> cells, as measured by MTS assay on commercial BN, BN nanoparticles, and BN nanosheets. Reproduced with permission from *Nano Res.*, 2017, **11**, 334–342 Copyright 2017 Springer.<sup>42</sup>

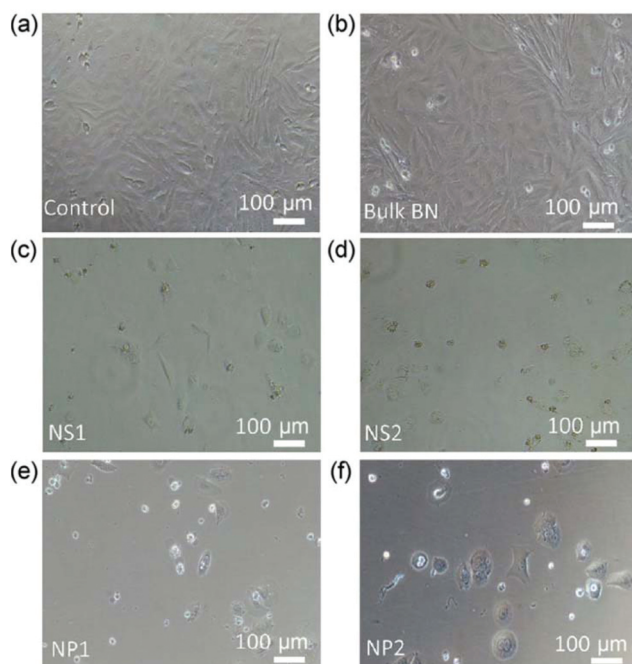


**Fig. 7** Bright-field microscopy images of SaOS<sub>2</sub> cells cultured in the presence of (a) standard culture medium (control), (b) bulk BN, (c) nanosheet NS1, (d) nanosheet NS2, (e) nanoparticle NP1, and (f) nanoparticle NP2. Reproduced with permission from *Nano Res.*, 2017, **11**, 334–342 Copyright 2017 Springer.<sup>42</sup>

Higher surface area would suggest more unsaturated boron atoms on the surface, whose high reactivity would induce the production of ROS species and explain the increasing toxicity for decreasing particle dimensions. An alternative reason suggested by the authors was that smaller nanoparticles are more effectively imported on the cells by phagocytosis, and then trigger the ROS formation. Irrespective of the type of mechanism by which nanoparticles act, this study further supports the notion that the size and shape of the boron nitride nanoparticles have a strong impact on its biocompatibility, in accord with,<sup>36,38,39</sup> this would also explain why similar sizes

for different shapes induce different responses in the tested cells, as could be noticed for the dimension of the nanosheets in this study and that of nanotubes in previous reports, where the material was found to be biocompatible, thanks to a lower number of unsaturated B atoms.

### Wetting/non-wetting behaviour of BN

As it has been realized from the literature that BN itself is fairly bio-compatible, the reported toxicity is arising from the coatings that are introduced on BN. This section describes the importance and effect of coatings on BN towards mammalian cells. Prior to this, it is worth mentioning that the wetting properties of BN play an important role in characterizing and identifying the appropriate coating material, which in turn plays an important role in performance. Like graphene, BN is weakly hydrophobic with a contact angle of 86°.<sup>44</sup> Interestingly, the BN contact angle range varies with the synthesis temperature.<sup>45</sup> This property of flexible tailoring during growth gives the feasibility to have BN nanosheets ranging from hydrophilic to super hydrophobic. In 2009, it was reported that partially vertically aligned BNNTs grown on silicon substrates are superhydrophobic compared to BN thin films.<sup>46</sup> Amir Pakdel *et al.*, have reported that the synthesis temperature range is directly proportional to the increase in contact angle. For synthesis temperatures of 900 °C to 1200 °C the reported contacted angles are in the range of 50° to 150°, respectively. The same authors in their next work have reported the tailoring of BN nanosheets from super hydrophilic to hydrophobic.<sup>47</sup> Interestingly, they have used previously synthesized superhydrophobic BN nanosheets (ref above) and films and altered their surface wetting properties by a one-step plasma process leading to grafting of functional groups (hydroxyl). This process not only makes it easier to determine the surface properties of BN sheets but also solves the dispersibility issues that were faced by many researchers. Similar works have been reported by several researchers which explains the wetting and non-wetting properties of BN films.<sup>48–52</sup>

### Importance of a coating

To the best of our knowledge, BN biocompatibility was first investigated by Ciofani *et al.* in 2008<sup>53,54</sup> with an evaluation of the impact of polyethyleneimine-wrapped boron nitride nanotubes (BNNTs) on neuroblastoma cells. The BNNTs, produced through ball milling and annealing,<sup>55</sup> were first coated with a polymer to attain a stable dispersion in aqueous suspension, and then tested with cells for up to 72 hours. Cell viability and replication retained relatively normal values up to a PEI-coated-BNNTs concentration of 5.0 μg mL<sup>-1</sup>, and then decreased to around 75% after 72 h. This shift was attributed to the coating, but not to the material itself. Cellular uptake of quantum dots attached to these nanotubes by endocytosis did not seem to have negative effects on cell function and morphology. Rather, the energy-dependent pathway identified for the nanotubes internalization might again be due to the PEI coating, rather than nanotubes itself.



In order to guarantee the dispersion of nano-dimension boron nitride compounds and avoid subsequent clustering caused by the natural hydrophobicity of the raw material, coatings are necessary. In fact, as proven in the case of carbon nanotubes, cytocompatibility results might depend not only on the material but also on the processing and final shape of the compound, where the latter would be strongly impacted in case of agglomeration. Based on their previous results, Ciofani *et al.*<sup>35</sup> suggested the use of BNNTs coated with poly-L-lysine (PLL) and investigated its interaction with C2C12 cells. BNNTs were produced through ball milling and annealing, to obtain nanotubes with an average length of 242 nm. As expected, these were dispersed in a stable aqueous solution using PLL. Conjugated quantum dots allowed the tracking of the material into the living cells. Overall, the cell viability and cell density were not different from the control, regardless of the concentration of PLL-BNNT tested. The achievement of confluence in all performed tests suggested that BNNT did not have any considerable impact on cellular replication. Interestingly, decrease in metabolic activity was observed when the cells were incubated with 3  $\mu\text{g mL}^{-1}$  solution of PLL only, suggesting that the surfactant may be toxic to some extent. With lower concentrations of PLL-coated-BNNTs, no significant membrane damage was observed in the cells, and a comparable to slightly increased value in protein content could be observed for cells undergoing differentiation. Through the combined use of quantum dots and sodium azide, it was possible to conclude that the mechanism of internalization of the nanotubes was energy-dependent.

As previously stated, the intrinsic inertness of BN compounds, in any shape, determines high hydrophobicity of the material and makes it difficult to disperse. This distinctive trait might strongly impact the results of biocompatibility assays both *in vitro* and *in vivo*, and this limitation needs to be overcome. Adoption of specific solutions such as surface coating and functionalization, both with covalent and non-covalent possibilities, can help in enhancing dispersion. This in turn would permit to exploit the better stability and surface zeta potential of BN in solution, both of which may impact the compatibility and internalization of the material.<sup>56,57</sup>

For example, Li *et al.*<sup>58</sup> coated BNNTs with silica in order to improve the stability of the suspension and to increase the loading and delivering efficiency of doxorubicin by controlling the surface zeta potential of the material. In this study, BNNTs were synthesized through CVD process<sup>33</sup> followed by oxidation and sonication to reduce the original size to around 1  $\mu\text{m}$ . This resulted in a stable suspension after 24 h, while the non-coated control sedimented after 3 h. After this, doxorubicin was loaded on both functionalized and non-functionalized BNNTs, to test how the loading and endocytosis efficiency changed with surface charge. Given that higher stability of the suspension enhances the uptake by cells, as does the positive surface charge of the particle, BNNTs functionalized with nanoporous silica with  $\text{NH}_2$  grafted on the surface proved to be a valid engineered tool for drug delivery into cells. They yielded superior results compared to simple mesoporous silica

functionalized BNNTs (stable but with a negative zeta potential) and non-functionalized BNNTs. Ulterior confirmation of these results was obtained by an *in vitro* study on prostate cancer cells that delivered confirmatory results. In conclusion, the coating did not only fulfill its original goal of improving the suspension stability, but actually played a key role in improving the drug loading ability and delivery efficiency.

Nithya *et al.*<sup>59</sup> confirmed that coating effectively helps with the suspension stability and can also be used to confer specific characteristics to BNNTs. In addition, the coating had an impact the final compatibility of the material.<sup>55</sup> In the cited article, the cytotoxicity of BNNTs coated with different polymers was examined. Specifically, the effect of pluronic P123, pluronic F127, polyethyleneimine and ammonium oleate coatings of nanotubes were examined on Vero and Chang cells, breast cancer cells and adenocarcinomic human alveolar basal epithelial cells.

A preliminary test revealed high toxicity of PEI starting from low concentrations. For the other polymers, the cell viability decreased to around 20% with increasing polymer concentration, with the notable exception of pluronic F127 that was far less toxic, even at concentrations as high as 1  $\text{mg mL}^{-1}$ . The nanotubes were then coated with the four different polymers and incubated for 24 h with the cells. Again, pluronic F127 was most bio-compatible, while PEI was most toxic. Interestingly, while both the pristine and pluronic F127 coated nanotubes were not toxic at concentrations lower than 250  $\mu\text{g mL}^{-1}$ , once loaded with anti-cancer drugs, a 50% death of cancerous cells was attained with nanotube concentrations lower than those necessary to free anticancer drugs to obtain the same results. The authors concluded<sup>34</sup> that even in case of biocompatible surfactants, as pluronic F127, pristine BNNTs do show a certain level of cytotoxicity above the concentration of 250  $\mu\text{g mL}^{-1}$ , and the surfactant shielding action is not effective in limiting the nanotubes toxicity above that concentration. In drug delivery applications drug-loaded BNNTs proved to have better efficacy compared to the administration of free drug.

Another way to remedy the hydrophobicity of BN may be to find alternative processing methods or subsequent treatments to make the material less hydrophobic, or even hydrophilic, thus allowing a better dispersion in solution. In this regard, an interesting example is provided by Li *et al.*,<sup>60</sup> regarding wettability of BNNT film. The said films were grown on substrates of steel using the boron ink method,<sup>61</sup> to a final thickness of 20–40  $\mu\text{m}$ . The films then underwent a  $\text{N}_2 + \text{H}_2$  gas plasma treatment using different modes, in order to impact the material surface. This changed the contact angle of the material from the original 158 degrees to a range from 60 to 5, according to different modes of plasma treatment, thus making the final product hydrophilic to super hydrophilic. In particular, the treatment with a conjugation of pulsed and continuous wave plasma led to a higher quantity of N-containing functional groups on the film surface. This, in turn, correlated with enhanced cell proliferation and viability of both human mammary fibroblast and transformed cell line tested on the BNNT samples (Fig. 8).



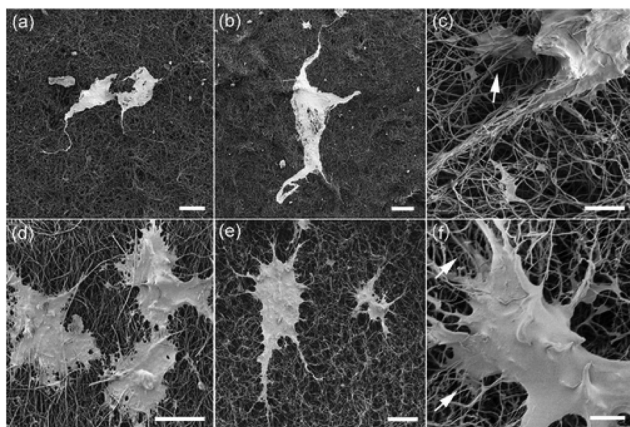


**Fig. 8** SEM images of fibroblasts on (a) untreated and (b and c) plasma treated BNNT films; and TXP RFP3 cells on (d) untreated and (e and f) plasma treated BNNT films. Scale bars: (a and b) 50  $\mu\text{m}$ ; (c) 5  $\mu\text{m}$ ; (d and e) 20  $\mu\text{m}$ ; (f) 5  $\mu\text{m}$ . Reproduced with permission from *J. Phys. Chem. C*, 2012, **116**, 18334–18339. Copyright 2012 ACS.<sup>60</sup>

A different approach aimed at improving the stability of boron nitride nanoparticles suspension was adopted by Weng *et al.*<sup>62</sup> In this study, BNs were obtained through an innovative solid reaction, where boric acid substructures substitute C atoms in graphitic carbon nitride thanks to a thermally activated process. This new processing method considerably increases the number of hydroxylic groups on the surface, and allows the formation of a stable water solution with boron nitrides up to a concentration of 2  $\text{mg mL}^{-1}$ , without the need for any surfactant.

The testing of boron nitride nanoparticles biocompatibility with mouse embryonic fibroblast cells and human prostate cancerous cells showed no adverse effect on either of the cell lines, with a viability superior to 90% for all concentrations tested up to 100  $\mu\text{g mL}^{-1}$ . Nanotubes loaded with doxorubicin were tested on human cancerous cells to evaluate the transport properties of drugs *in vitro*: results showed a loading capacity dependent on the duration of the solubilization treatment. In addition, higher toxicity on cancerous cells in case of DOX wrapped with hydroxylated BNs with respect to free doxorubicin was observed, presenting the final product as a good candidate for drug delivery applications.

### Applications in composites

Superior mechanical properties of BN nanotubes have led to their use in a number of composites. A very common use of BN nanostructure/compounds has been as a reinforcing phase in composites, some of which with biomedical applications. This necessitated an investigation of cytotoxicity of the composites enhanced by BNNTs.<sup>63,64</sup>

In 2010, Lahiri *et al.* designed a biodegradable polylactide-polycaprolactone copolymer reinforced with BNNTs to be employed as a scaffold in tissue engineering.<sup>65</sup> Given the biodegradability of the matrix, it is extremely relevant that the reinforcing phase is biocompatible, considering the long-time

permanence of the scaffold in the tissues. In this study, the NTs had a final length ranging from 0.43 to 5.8  $\mu\text{m}$  and a mean diameter of 71 nm. In addition to a noteworthy enhancement of both tensile strength and elongation, cytotoxic analysis on osteoblasts and macrophages did not underline any remarkable cytotoxic effect. On the contrary, BNNTs addition to the matrix granted a change in osteoblast cell morphology, slightly more lens shaped, and accelerated growth and differentiation. The authors argued that this effect was due to the natural affinity of BNNT for proteins. A similar approach was adopted by Lahiri *et al.* in a subsequent study,<sup>66</sup> where BNNTs were used to reinforce hydroxyapatite (HA). In this case, BNNTs had a length ranging from 0.43 to 5.8  $\mu\text{m}$  and a mean diameter of 71 nm, with slightly different shapes. This time the composite was obtained through spark plasma sintering, after a homogenous mixing of the precursor powders through ultrasonication. The viability of osteoblasts on HA-BNNT did not noticeably differ from the control of HA only, while proliferation and differentiation were enhanced. The authors suggested that this is due to the natural affinity of BNNTs toward proteins, whose attachment on the BNNTs surface might assist the proliferation of osteoblasts.

In addition to the mentioned mechanical properties, used for strengthening composites, the piezoelectric behaviour of BN nanotubes means they could be used for cell stimulation. Ciofani *et al.*<sup>67</sup> examined the effects of BNNT nanovectors on neuronal-like cells. In this study, NTs of 200–600 nm in length<sup>41</sup> were dispersed with glycol-chitosan, which provided a non-covalent wrapping of the material to permit a better stability of the suspension. A preliminary test conducted to evaluate the biocompatibility of the material showed no difference in cell viability compared to controls up to concentrations of 50  $\mu\text{g mL}^{-1}$ . Until the 9<sup>th</sup> day of exposition, there was no sign of ROS formation, apoptosis, nor any relevant change in terms of cellular differentiation. TEM imaging confirmed previous observations of nanotubes internalized in the cytoplasm and contained in vesicles. When nanotubes underwent ultra sound stimulation, thus expressing their piezoelectric behaviour, cells were electrically stimulated. This led to an increase in the number and length of neurites, and in the number of neuronal processes per differentiated cell.

Danti *et al.*<sup>68</sup> investigated the interactions of BN nanotubes with human mesenchymal cells of different origins. In addition to the absence of relevant toxicity on the cells, TEM images confirmed the phagocytosis of the material inside the cell cytoplasm. These findings were further corroborated by a later study by the same group,<sup>69</sup> where BNNTs taken up by osteoblast cells were stimulated through low frequency ultrasounds. BNNTs with a length inferior to 500 nm were obtained through a milling and annealing method<sup>70</sup> and coated with poly-L-lysine in order to attain a stable suspension. To test cell viability and define the optimal concentration that would combine least toxicity with effective cell stimulation, media containing PLL-coated BN nanotubes in various concentrations were incubated with human osteoblastic cells up to three days. No cytotoxicity, apoptosis or necrosis was detected,



and a concentration of  $10 \mu\text{g mL}^{-1}$  was found to be optimal. The presence of BNNTs alone, engulfed by phagocytosis, seemed to increase the maturation of osteoblasts. Mineralization of osteoblast was triggered specifically with ultra sound stimulation. Aside from the improvement of mechanical properties provided by the use of BN as second phase and the possibility the exploitation of its piezoelectric properties open, boron nitride can also be used for other purposes.

In a study by Li *et al.*,<sup>71</sup> interaction of a BN nanotubes layer with mesenchymal cells was evaluated. The 2D material was obtained by chemical vapor deposition,<sup>33,72</sup> followed by a secondary treatment in order to purify and shorten<sup>73</sup> the resulting nanotubes to an average length of around 1–2  $\mu\text{m}$ . Interestingly, the BNNT layer seemed to improve both cellular attachment and protein adsorption, and fluorescent analysis disclosed how cells cultivated in contact with the BN layer had better attachment and spreading on the surface with respect to the control on simple glass. In particular, it was observed that there is an enhanced cell proliferation over the test period for a concentration of  $5 \mu\text{g mL}^{-1}$ , and a higher secretion of proteins specific for osteogenic differentiation is identifiable for the said concentration with respect to the controls over the same lapse of time (Fig. 9).

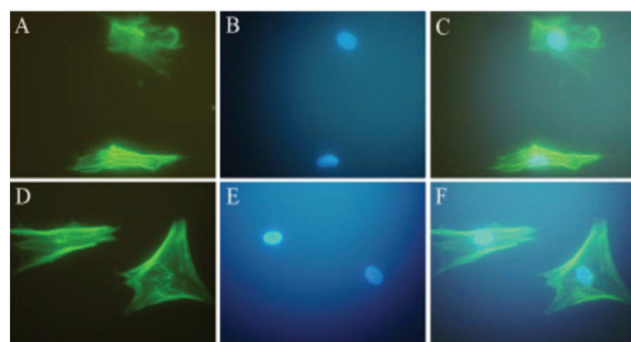


**Fig. 9** Left: Fluorescent images of MSCs after 24 h of culture with control (A–C) and BNNTs layer at  $2 \mu\text{g mL}^{-1}$  (D–F); Right: Quantification of cell attachment area of MSCs after 24 h of culture with control and BNNTs layer at  $2 \mu\text{g mL}^{-1}$  ( $n = 80$ ). Reproduced with permission from *J. Biomed. Mater. Res., Part B*, 2016, **104**, 323–329. Copyright 2016 John Wiley and Sons.<sup>71</sup>

Analogously, Farshid *et al.*<sup>74</sup> attempted to construct a polymeric matrix composite useful for tissue engineering, with a reinforcing second phase of BN. Their study was mostly related to comparing the change in mechanical properties and interaction with cells in case of different shapes of the material, specifically nanotubes and nanoplatelets.

To create the composite, polypropylene fumarate, a biodegradable polymer with extensive use in biomedical applications, was mixed with *N*-vinyl pyrrolidone, a crosslinker, and 0.2% w/w of boron nitride nanoplatelets or nanotubes. The addition of a second phase increased both the Young's modulus and the compressive yield strength compared to the polymeric control only, particularly in case of addition of NPs, for which the increase was 38% and 31%, respectively for the two cited mechanical properties. Raw Polypropylene fumarate was tested in multiple conditions with boron nitride particles/platelets concentrations, before and after crosslinking and in its degradation products within the system.

Overall, the composite showed good biocompatibility, with a cell viability dependent on the second phase concentration. The cell viability for raw material dispersions with concentrations up to  $100 \mu\text{g mL}^{-1}$  was above 73%, and it was further enhanced in the composite form, where the viability rose to 79% and above. In addition, acceptable levels of cellular attachment and normal cellular morphology were reported. The toxicity of the degradation products exhibited a dose dependent behaviour.

#### Toxicology *in vivo*

Up to date, *in vivo* toxicology results on BN are very limited. Ciofani *et al.*<sup>75</sup> reported the first pilot investigation on BNNTs, injecting a single dose of 2 mL of solution with a concentration of  $1 \text{ mg mL}^{-1}$  of BNNTs coated with G-chitosan in the marginal ear vein of male rabbits. BNNTs were produced according to the process already adopted by the same group.<sup>41</sup> FIB images show a final length of the nanotubes comprised between 0.5 and 2.0  $\mu\text{m}$ , and a diameter between 30 and 100 nm. At time points of 0, 2, 4, 24 and 72 hours, blood analysis was performed and out of ordinary behaviour, such as sweating and trembling, was monitored. No change in behaviour was noticed during the entire period. Blood analysis values did not differ significantly from those of the controls injected with chitosan only, with the exception of the platelets count, which was higher in the presence of BNNTs after 72 h. The same group reported a follow-up study,<sup>76</sup> increasing the dosage, prolonging the monitoring time to 7 days and testing possible differences in case of multiple injections. In this study, the mean length of the nanotubes was around 500 nm. Again, no behavioural change was detected for the entire period of observation, regardless of the dose or the injection pattern. Blood samples, collected 0, 1, 3 and 7 days after injection, did not show any significant differences with respect to controls. Moreover, a preliminary analysis of the pharmacokinetic behaviour of the material showed a good distribution in the body, with rapid clearance from the blood. It is unclear whether this is related to the nanotubes themselves, or the





Table 1 Correlation between the type of boron nitride, production method, concentration and time of exposure on different cells and their responses

BN form	Production method	BNNT geometry	Dispersion agent	Cell type	Max concentration of exposure	Time of exposure (hours)	Results	Ref.
BNNTs	Ball milling and annealing	—	Polyethyleneimine	Neuroblastoma cells	5 $\mu\text{g mL}^{-1}$	72	Non cytotoxic	22
BNNTs	CVD	Multiwalled, length <10 nm, $D$ 20–30 nm	None	Kidney cells	100 mg $\text{mL}^{-1}$	96	Non cytotoxic, aggregated	27
BNNTs	Ball milling and annealing	$L$ 200–300 nm	Poly-L-lysine	Myoblast cells	15 $\mu\text{g mL}^{-1}$	72	Non cytotoxic, optimal cell viability up to 10 $\mu\text{g mL}^{-1}$ , metabolic decrement at 72 h at conc. of 15 $\mu\text{g mL}^{-1}$	30
BNNTs	CVD	Multiwalled, $L \sim 10 \mu\text{m}$ , $D < 80 \text{ nm}$	Tween 80	Human lung adenocarcinoma epithelial cells, human embryonic kidney cells, murine embryonic fibroblast cells and murine alveolar macrophage cells	20 $\mu\text{g mL}^{-1}$	120	Cytotoxic already at 2 $\mu\text{g mL}^{-1}$ , metabolic and morphological change in cells	31
BNNTs	CVD + homogeneization + sonication	Multiwalled, $L \sim 1.5 \mu\text{m}$ , $D$ 10–80 nm	Gum Arabica	Neuroblastoma cells and human umbilical vein epithelial cells	100 $\mu\text{g mL}^{-1}$	72	Non-cytotoxic up to 20 $\mu\text{g mL}^{-1}$ , cytotoxic for concentrations of 50 and 100 $\mu\text{g mL}^{-1}$	54
BNNTs	High-temperature synthesis	Both single and small aggregates of nanotubes, bamboo-like, $L$ 200–600 nm, $D \sim 50 \text{ nm}$	Glycol-chitosan	Neuroblastoma human cells	100 $\mu\text{g mL}^{-1}$	48	Non-cytotoxic up to 20 $\mu\text{g mL}^{-1}$ , slight viability decrease for conc. >50 $\mu\text{g mL}^{-1}$	32
BNNTs	CVD	Multiwalled, straight, tubular, inner $D \sim 10$ , outer $D \sim 25 \text{ nm}$	None	Vero and Chang cells	1000 $\mu\text{g mL}^{-1}$	24	Non cytotoxic, good viability up until 250 $\mu\text{g mL}^{-1}$	39
BNNTs	CVD	Multiwalled, straight, tubular, inner $D \sim 10$ , outer $D \sim 25 \text{ nm}$	Pluronic P123	Vero cells	1000 $\mu\text{g mL}^{-1}$	24	Non-cytotoxic, IC50 125 $\mu\text{g mL}^{-1}$ (for vero 250 is 40% viab)	39
BNNTs	CVD	Multiwalled, straight, tubular, inner $D \sim 10$ , outer $D \sim 25 \text{ nm}$	Pluronic P123	Chang cells	1000 $\mu\text{g mL}^{-1}$	24	non-cytotoxic, IC50 125 $\mu\text{g mL}^{-1}$ (50% cells still alive)	39
BNNTs	CVD	Multiwalled, straight, tubular, inner $D \sim 10$ , outer $D \sim 25 \text{ nm}$	Pluronic F127	Vero cells	1000 $\mu\text{g mL}^{-1}$	24	Non-cytotoxic up until 500 (IC <i>circa</i> 500), cell viability above 30% at 1000 $\mu\text{g mL}^{-1}$	39
BNNTs	CVD	Multiwalled, straight, tubular, inner $D \sim 10$ , outer $D \sim 25 \text{ nm}$	Pluronic F127	Chang cells	1000 $\mu\text{g mL}^{-1}$	24	Non-cytotoxic, 70% cell viability even at 1000 $\mu\text{g mL}^{-1}$	39
BNNTs	CVD	Multiwalled, straight, tubular, inner $D \sim 10$ , outer $D \sim 25 \text{ nm}$	Polyethyleneimine	Vero and Chang cells	1000 $\mu\text{g mL}^{-1}$	24	Cytotoxic already at 7.8 $\mu\text{g mL}^{-1}$	39
BNNTs	CVD	Multiwalled, straight, tubular, inner $D \sim 10$ , outer $D \sim 25 \text{ nm}$	Ammonium oleate	Vero cells	1000 $\mu\text{g mL}^{-1}$	24	Non-cytotoxic, IC50 >125 $\mu\text{g mL}^{-1}$	39
BNNTs	CVD	Multiwalled, straight, tubular, inner $D \sim 10$ , outer $D \sim 25 \text{ nm}$	Ammonium oleate	Chang cells	1000 $\mu\text{g mL}^{-1}$	24	Non-cytotoxic, IC50 250 $\mu\text{g mL}^{-1}$	39



Table 1 (Contd.)

BN form	Production method	BNNT geometry	Dispersion agent	Cell type	Max concentration of exposure	Time of exposure (hours)	Results	Ref.
BNNTs film	Boron ink method	Bamboo-like and cylindrical NTs, 20–40 μm thick film	Plasma treated	Human mammary fibroblast, transformed breast tumor cells	$1 \times 10^5$ cells on a 35 mm diameter cell culture plate	48 (breast tumor cells) and 96 (fibroblasts)	Non-cytotoxic, cell proliferation on the film enhanced with plasma treatment	40
BNNTs	Commercial	Cylindrical and bamboo-like structures, $L$ 0.43–5.8 μm, $D$ 32–145 nm	None	Osteoblasts and macrophages	$1 \mu\text{g mL}^{-1}$	60	Non-cytotoxic, normal cell growth	57
BNNTs	Spark plasma sintering	$L \sim 0.43$ – $5.8$ μm, mean $D$ 71 nm	2nd phase in HA	Human osteoblasts	4 wt%	120	Non-cytotoxic, normal cell growth	58
BNNTs	Annealing method	Single and aggregate, bamboo-like structure, $L$ 200–600 nm, $D \sim 50$ nm	Glycol-chitosan	Nuronal-like cells (PC12)	$100 \mu\text{g mL}^{-1}$	216	Non-cytotoxic, no difference with control up to a concentration of $50 \mu\text{g mL}^{-1}$	59
BNNTs	Milling and annealing	$L < 500$ nm, $D$ 40–70 nm	Poly-L-lysine	Osteoblast cells	$15 \mu\text{g mL}^{-1}$	72	Non-cytotoxic	61
BNNTs layer	CVD + shortening + oxidation	$L$ 1–2 μm	None	Mesenchymal stem cells	$25 \mu\text{g mL}^{-1}$	336	Non-cytotoxic, improve both cellular attachment and protein adsorption at $5 \mu\text{g mL}^{-1}$ after 14 days	63
BNNTs	Commercial	Bamboo-like structure, $L$ 0.5–2.0 μm, $D$ 30–100 nm	Glycol-chitosan	<i>In vivo</i>	2 mL of a $1 \text{ mg mL}^{-1}$	72	Non-cytotoxic, higher platelet count	67
BNNTs	Commercial	$L \sim 500$ nm	Glycol-chitosan	<i>In vivo</i>	$10 \text{ mg kg}^{-1}$	168	Non-cytotoxic, no alteration in blood values or behavior at any concentration	68
BNNTs	CVD + shortening	Crystalline, multiwalled, $L$ 1.0–2.5 μm, $D$ 10–80 nm	Gum arabica	<i>In vivo</i>	Single injection, $200 \mu\text{g g}^{-1}$	24	Non-cytotoxic	69
BNNTs	CVD + shortening	Crystalline, multiwalled, $L$ 1.0–2.5 μm, $D$ 10–80 nm	Gum arabica	<i>In vivo</i>	Multiple injections, final quantity $200 \mu\text{g g}^{-1}$	336	Non-cytotoxic	69
BNNSS	Ballmilling in ammonia	$1 \mu\text{m } D \times 100 \text{ nm}$ in thickness	None	Human osteosarcoma cells	$1 \text{ mg mL}^{-1}$	168	Non-cytotoxic	34
BNNSS	Ballmilling in ammonia	$100 \text{ nm } D \times 3 \text{ nm}$ in thickness	None	Human osteosarcoma cells	$1 \text{ mg mL}^{-1}$	168	Cytotoxic	34
BNNPS	Ballmilling in argon	Spherical, amorphous-like, $D$ 100–200 nm	None	Human osteosarcoma cells	$1 \text{ mg mL}^{-1}$	168	Cytotoxic, the more the lower the $D$	34
Boron nitrides	Solid reaction method	Branched nanoribbons, hydroxylated layered structure	—	Mouse embryonic fibroblast cells and human prostate cancerous cell	$100 \mu\text{g mL}^{-1}$	24	Non-cytotoxic	42



**Table 2** Correlation between the type of graphene, concentration and time of exposure on different bacteria/mammalian cells and their responses

Graphene form	Cell type	Max concentration of exposure ( $\mu\text{g ml}^{-1}$ )	Time of exposure (hours)	Result	Ref.
GO/rGO	<i>E. coli</i>	40	2	Antibacterial	81
GO/rGO	<i>E. coli</i> (DH5 $\alpha$ )	85	2	Antibacterial	82
GO	<i>E. coli</i>	75	16	Biocompatible	83
GO	Mouse embryo fibroblasts 3T3	1	48	Biocompatible	84
GO	HeLa cells	10	48	Biocompatible	85
GO	Human lymphoblastic leukemia	10	24	Biocompatible	86
GO	MCF7-human breast cancer				
GO	Human adipose stem cells	0.024%	24	Biocompatible	80
Pristine graphene monolayer	L929 fibroblasts	—	48	Biocompatible	87
Graphene film doped with Ag nanoparticles	<i>E. coli</i> and mouse osteoblast-like MC3T3-E1 cells	148 mg of AgNO <sub>3</sub> which corresponds to the mass ration of graphene	24/7 days	Antibacterial/biocompatible	88

surface coating. If the last assumption was correct, that would also accord the possibility of controlling the permanence of the coated nanotubes inside the body with the use of different coatings, in order to best fit the requirements of their eventual application, may it be short or long-termed.

In the latest report on the topic, Salvetti *et al.* tested the compatibility of BNNTs on planarians.<sup>77</sup> Multi-walled BNNTs were fabricated through a CVD process,<sup>72</sup> then underwent a shortening and stabilization process<sup>43</sup> to deliver nanotubes with an average length of 1.5  $\mu\text{m}$ , which were eventually coated with gum arabic. Different doses and number of injections were chosen in order to evaluate the toxicity in case of acute and chronic exposures. In this case too, no behavioural change was detected after the injections. No morphological change or DNA damage in cells was detected either, and no sign of nanotubes was found three days after the last injection. In conclusion, BNNTs did not prove to be cytotoxic when tested *in vivo* on planarians, while the coating may reduce the possible toxicity of the raw material. The possible dissolution of the non-covalent surface coating after the endocytosis, due to intrinsic inertness, suggests that the raw material itself would not cause any significant damage. Further investigations are necessary, since the *in vivo* trials conducted thus far are only a starting point.

### Antibacterial properties

Antibacterial properties of BN have not been thoroughly investigated. In the study by Nithya *et al.*,<sup>59</sup> pristine BNNTs and BNNTs functionalized with different kinds of polymers were tested on *Escherichia coli* and *Staphylococcus aureus*. Raw material did not have any bactericidal effect. The authors argue that this is due to the intrinsic hydrophobicity of the nanotubes and weak interactions between OH groups and BN, which would prevent effective interaction with the bacteria. As previously observed, pristine PEI exhibited a strong antibacterial effect, while the other tested polymers were harmless to bacteria.<sup>78</sup> When used as coatings, the same pattern emerged with the tested polymers. No significant decrease in bacterial optical density was observed for pluronic P123, pluronic F127 and ammonium oleate coated nanotubes, while PEI-coated

BNNTs were bactericidal. From these observations, it can be concluded that BNNTs do not seem to have inherent bactericidal effect, and any antibacterial activity observed was due to the coating. By contrast, according to the research conducted by Parra *et al.*,<sup>79</sup> hexagonal BN could be used to prevent the biocorrosion of copper substrates by *Escherichia coli*. After 24 hours of incubation with BN coated copper sample, bacteria viability came up to 118%, indicating that not only the BN itself does not seem to have any inherent antibacterial ability, but also that it would prevent harming copper ions to interact with the bacteria deposited on the surface. The result is interesting, especially considering that bacterial adhesion results enhanced in the case of hexagonal BN coating with respect to the untreated substrate. A study<sup>80</sup> shows that when boron (NaB is the source) was integrated with graphene oxide, there is an enhancement in cell attachment and proliferation. It would be worth investigating whether the BN itself is required for this effect, or any other boron source could also enhance the cell proliferation.

### Conclusion

Here we propose that BN could be an interesting alternative to graphene-based materials when it comes to bio-applications. Table 1 sums up all the studies reported on BN biocompatibility. Table 2<sup>80–88</sup> presents the findings from some key studies on biocompatibility of graphene-based materials. Overall, these studies have been performed with similar concentrations and exposure times, and they suggest that BN biocompatibility is comparable to that of carbon-based 2D materials. Nevertheless, more is needed to be done to characterize the impact of these 2D materials on/in living systems. Different forms of BN and carbon-based 2D materials differ considerably in processing methods, the degree of material purity, its size, shape and thickness of structure. Moreover, in case of BN, the use of various coatings and surface treatments makes it harder to compare the studies and identify equivocal thresholds for time of exposure and maximum doses. It should be noted that similar material processing and morphology cannot be expected to deliver the same results on all



cells lines, given the cellular specialization. Though the literature that is presented here reveals some overall contradictory results, it has to be noted that this contradiction is coming from the coatings/surfactants that are used along with BN but not from pristine BN itself. Unlike other carbon nanomaterials where the flake size, preparation method, shape and working conditions play an important role in determining the toxicity or bio-compatibility, the pristine forms of BN without coatings turn out to be bio-compatible *in vitro* and *in vivo*. This can project BN as a baseline 2D material for bio-applications and once the clinical guidelines get defined for the most relevant biocompatibility parameters, different strategies can be adopted to engineer the BN nanostructures for specific applications like imaging, drug delivery and stimulation.

## Conflicts of interest

There are no conflicts to declare.

## Acknowledgements

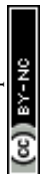
The authors would like to acknowledge funding from the Olle Engqvist Foundation (Project no. 28240025), the Vinnova SIO Grafen and the Chalmers University of Technology.

## References

- 1 F. P. Bundy and R. H. Wentorf, *J. Chem. Phys.*, 1963, **38**, 1144–1149.
- 2 F. R. Corrigan and F. P. Bundy, *J. Chem. Phys.*, 1975, **63**, 3812–3820.
- 3 L. Vel, G. Demazeau and J. Etourneau, *Mater. Sci. Eng., B*, 1991, **10**, 149–164.
- 4 Q. Weng, X. Wang, X. Wang, Y. Bando and D. Golberg, *Chem. Soc. Rev.*, 2016, **45**, 3989–4012.
- 5 A. Pakdel, Y. Bando and D. Golberg, *Chem. Soc. Rev.*, 2014, **43**, 934–959.
- 6 X. Blasé, A. Rubio, S. G. Louoe and M. L. Cohen, *Europhys. Lett.*, 1994, **28**, 335–340.
- 7 J. Wang, C. H. Lee and Y. K. Yap, *Nanoscale*, 2010, **2**, 2028–2034.
- 8 D. Golberg, P. M. F. J. Costa, O. Lourie, M. Mitome, X. Bai, K. Kurashima, C. Zhi, C. Tang and Y. Bando, *Nano Lett.*, 2007, **7**, 2146–2151.
- 9 E. R. Hernandez, C. Goze, P. Bernier and A. Rubio, *Phys. Rev. Lett.*, 1998, **80**, 4502.
- 10 A. P. Suryavanshi and M. Yu, *Appl. Phys. Lett.*, 2004, **84**, 2527.
- 11 N. G. Chopra and A. Zettl, *Solid State Commun.*, 1998, **105**, 297–300.
- 12 C. W. Chang, *Appl. Phys. Lett.*, 2005, **86**, 173102.
- 13 A. Zettl, C. W. Chang and G. Begtrup, *Phys. Status Solidi B*, 2007, **244**, 4181–4183.
- 14 Y. Chen, J. Zou, S. J. Campbell and G. Le Caer, *Appl. Phys. Lett.*, 2004, **84**, 2430–2432.
- 15 Y. Dai, W. Guo, Z. Zhang, B. Zhou and C. Tang, *J. Phys. D: Appl. Phys.*, 2009, **42**, 085403; G. Ciofani, V. Raffa, A. Menciacsi and A. Cuschieri, *Nano Today*, 2008, **4**, 8–10.
- 16 G. Oostingh, E. Casals, P. Italiani, R. Colognato, R. Stritzinger, J. Ponti, T. Pfaller, Y. Kohl, D. Ooms, F. Favilli, H. Leppens, D. Lucchesi, F. Rossi, I. Nelissen, H. Thielecke, V. F. Puentes, A. Dusch and D. Boraschi, *Part. Fibre Toxicol.*, 2011, **8**, 8.
- 17 T. Habib, D. S. Devarajan, F. Khabaz, D. Parviz, T. C. Achee, R. Khare and M. J. Green, *Langmuir*, 2016, **32**, 11591–11599.
- 18 X. Li, Q. Li and G.-X. Chen, *Mater. Lett.*, 2014, **134**, 38–41.
- 19 A. Chae, S.-J. Park, B. Min and I. In, *Mater. Res. Express*, 2018, **5**, 015036.
- 20 A. Falin, Q. Cai, E. J. G. Santos, D. Scullion, D. Qian, R. Zhang, Z. Yang, S. Huang, K. Watanabe, T. Taniguchi, M. R. Barnett, Y. Chen, R. S. Ruoff and L. H. J. Li, *Nat. Commun.*, 2017, **8**, 15815.
- 21 D. Deepika, L. H. Li, A. M. Glushenkov, S. K. Hait, P. Hogdson and Y. Chen, *Sci. Rep.*, 2014, **4**, 7288.
- 22 X.-F. Jiang, Q. Weng, X.-B. Wang, X. Li, J. Zhang, D. Golberg and Y. Bando, *J. Mater. Sci. Technol.*, 2015, **31**, 589–598.
- 23 L. H. Li, J. Cervanka, K. Watanabe, T. Taniguchi and Y. Chen, *ACS Nano*, 2014, **8**, 1457–1462.
- 24 L. H. Li, T. Xing and Y. Chen, *Adv. Mater. Interfaces*, 2014, **1**, 1300132.
- 25 L. H. Li and Y. Chen, *Adv. Funct. Mater.*, 2016, **26**, 2594–2608.
- 26 M. Butts, M. Sinha, S. E. Genovese and M. Yamada, *United States patent US 20070207101A1*, 2007.
- 27 S.-H. Jhi and Y.-K. Kwon, *Phys. Rev. B: Condens. Matter Mater. Phys.*, 2004, **69**, 245407.
- 28 R. Ma, Y. Bando, H. Zhu, T. Sato, C. Xu and D. Wu, *J. Am. Chem. Soc.*, 2002, **124**, 7672–7673.
- 29 S. Syama and P. V. Mohanan, *Int. J. Biol. Macromol.*, 2016, **86**, 546–555.
- 30 A. M. Pinto, I. C. Goncalves and F. D. Magalhaes, *Colloids Surf., B*, 2013, **111**, 188–202.
- 31 J. Kim and S. Gurunathan, *Int. J. Nanomed.*, 2016, **11**, 1927–1945.
- 32 X. Chen, P. Wu, M. Rousseas, D. Okawa, Z. Gartner, A. Zettl and C. R. Bertozzi, *J. Am. Chem. Soc.*, 2009, **131**, 890–891.
- 33 C. Tang, Y. Bando, T. Sato and K. Kurashima, *Chem. Commun.*, 2002, **12**, 1290–1291.
- 34 P. Wu, X. Chen, N. Hu, U. C. Tam, O. Blixt, A. Zettl and C. R. Bertozzi, *Angew. Chem., Int. Ed.*, 2008, **47**, 5022–5025.
- 35 G. Ciofani, L. Ricotti, S. Danti, S. Moscato, C. Nesti, D. D'Alessandro, D. Dinucci, F. Chiellini, A. Pietrabissa, M. Petrini and A. Menciacsi, *Int. J. Nanomed.*, 2010, **5**, 285–298.
- 36 L. Horváth, A. Magrez, D. Golberg, C. Zhi, Y. Bando, R. Smajda, E. Horváth, L. Forró and B. Schwaller, *ACS Nano*, 2011, **5**, 3800–3810.



- 37 L. Horváth, A. Magrez, L. Forró and B. Schwaller, *Phys. Status Solidi B*, 2010, **247**, 3059–3062.
- 38 G. Ciofani, S. Del Turco, A. Rocca, G. de Vito, V. Cappello, M. Yamaguchi, X. Li, B. Mazzolai, G. Basta, M. Gemmi, V. Piazza, D. Golberg and V. Mattoli, *Nanomedicine*, 2014, **9**, 773–788.
- 39 S. Kang, M. Herzberg, D. F. Rodrigues and M. Elimelech, *Langmuir*, 2008, **24**, 6409–6413.
- 40 G. Ciofani, S. Danti, D. D'Alessandro, S. Moscato and A. Menciassi, *Biochem. Biophys. Res. Commun.*, 2010, **394**, 405–411.
- 41 J. Wang, Y. Gu, L. Zhang, G. Zhao and Z. Zhang, *J. Nanomater.*, 2010, 540456.
- 42 S. Mateti, C. S. Wong, Z. Liu, W. Yang, Y. Li, L. H. Li and Y. Chen, *Nano Res.*, 2017, **11**, 334–342.
- 43 T. Xing, S. Mateti, L. H. Li, F. Ma, A. Du, Y. Gogotsi and Y. Chen, *Sci. Rep.*, 2016, **6**, 35532.
- 44 H. Li and X. C. Zheng, *ACS Nano*, 2012, **6**, 2401–2409.
- 45 A. Pakdel, C. Zhi, Y. Bando, T. Nakayama and D. Golberg, *ACS Nano*, 2011, **5**, 6507–6515.
- 46 C. H. Lee, J. Drelich and Y. K. Yap, *Langmuir*, 2009, **25**, 4853–4860.
- 47 A. Pakdel, Y. Bando and D. Golberg, *ACS Nano*, 2014, **8**, 10631–10639.
- 48 R. C. Dutta, S. Khan and J. K. Singh, *Fluid Phase Equilib.*, 2011, **302**, 310–315.
- 49 A. Pakdel, X. Wang, Y. Bando and D. Golberg, *Acta Mater.*, 2013, **61**, 1266–1273.
- 50 A. Pakdel, Y. Bando, D. Shtansky and D. Golberg, *Surf. Innovations*, 2013, **1**, 32–39.
- 51 Y. Shi, C. Hamsen, X. Jia, K. K. Kim, A. Reina, M. Hofmann, A. L. Hsu, K. Zhang, H. Li, Z.-Y. Juang, M. S. Dresselhaus, L.-J. Li and J. Kong, *Nano Lett.*, 2010, **10**, 4134–4139.
- 52 X. Li, H. Qiu, X. Liu, J. Yin and W. Guo, *Adv. Funct. Mater.*, 2016, **27**, 1603181.
- 53 G. Ciofani, V. Raffa, A. Menciassi and A. Cuschieri, *Nano Today*, 2009, **4**, 5–10.
- 54 G. Ciofani, V. Raffa, A. Menciassi and A. Cuschieri, *Biotechnol. Bioeng.*, 2008, **4**, 850–858.
- 55 Y. Chen, F. Gerald, J. S. Williams and S. Bulcock, *Chem. Phys. Lett.*, 1999, **299**, 260–264.
- 56 S. E. Gratton, P. A. Ropp, P. D. Pohlhaus, J. C. Luft, V. J. Madden, M. E. Napier and J. M. DeSimone, *Proc. Natl. Acad. Sci. U. S. A.*, 2008, **105**, 11613–11618.
- 57 M. Motskin, D. M. Wright, K. Muller, N. Kyle, T. G. Gard, A. E. Porter and J. N. Skepper, *Biomaterials*, 2009, **30**, 3307–3317.
- 58 X. Li, C. Zhi, N. Hanagata, M. Yamaguchi, Y. Bando and D. Golberg, *Chem. Commun.*, 2013, **49**, 7337–7339.
- 59 J. S. M. Nithya and A. Pandurangan, Aqueous dispersion of polymer coated boron nitride nanotubes and their antibacterial and cytotoxicity studies, *RSC Adv.*, 2014, **4**, 32031–32046.
- 60 L. Li, L. H. Li, S. Ramakrishnan, X. J. Dai, K. Nicholas, Y. Chen, Z. Chen and X. Liu, *J. Phys. Chem. C*, 2012, **116**, 18334–18339.
- 61 L. H. Li, Y. Chen and A. M. Glushenkov, *J. Mater. Chem.*, 2010, **20**, 9679–9683.
- 62 Q. Weng, B. Wang, X. Wang, N. Hanagata, X. Li, D. Liu, X. Wang, X. Jiang, Y. Bando and D. Golberg, *ACS Nano*, 2014, **8**, 6123–6130.
- 63 W. Meng, Y. Huang, Y. Fu, Z. Wang and C. Zhi, *J. Phys. Chem. C*, 2014, **2**, 10049–10061.
- 64 C.-K. Yang, *Comput. Phys. Commun.*, 2011, **182**, 39–42.
- 65 D. Lahiri, F. Rouzaud, T. Richard, A. K. Keshri, S. R. Bakshi, L. Kos and A. Agarwal, *Acta Biomater.*, 2010, **6**, 3524–3533.
- 66 D. Lahiri, V. Singh, A. P. Benaduce, S. Seal, L. Kos and A. Agarwal, *J. Mech. Behav. Biomed. Mater.*, 2011, **4**, 44–56.
- 67 G. Ciofani, S. Danti, D. D'Alessandro, L. Ricotti, S. Moscato, G. Bertoni, A. Falqui, S. Berrettini, M. Petrini, V. Mattoli and A. Menciassi, *ACS Nano*, 2010, **4**, 6267–6277.
- 68 S. Danti, A. Rocca, S. Moscato, S. Barachini, M. Petrini and G. Ciofani, *Ital. J. Anat. Embryol.*, 2012, **117**, 56.
- 69 S. Danti, G. Ciofani, S. Moscato, D. D'Alessandro, E. Ciabatti, C. Nesti, R. Brescia, G. Bertoni, A. Pietrabissa, M. Lisanti, M. Petrini, V. Mattoli and S. Berrettini, *Nanotechnology*, 2013, **24**, 465102.
- 70 J. Yu, Y. Chen, R. Wuhler, Z. Liu and S. P. Ringer, *Chem. Mater.*, 2005, **17**, 5172–5176.
- 71 X. Li, X. Wang, X. Jiang, M. Yamaguchi, A. Ito, Y. Bando and D. Golberg, *J. Biomed. Mater. Res., Part B*, 2016, **104**, 323–329.
- 72 C. Zhi, Y. Bando, C. Tan and D. Golberg, *Solid State Commun.*, 2005, **135**, 67–70.
- 73 C. Zhi, N. Hanagata, Y. Bando and D. Golberg, *Chem. – Asian J.*, 2011, **6**, 2530–2535.
- 74 B. Farshid, G. Lalwani, M. Shir Mohammadi, J. Simonsen and B. Sitharaman, *J. Biomed. Mater. Res., Part B*, 2017, **105**, 406–419.
- 75 G. Ciofani, S. Danti, G. G. Genchi, D. D'Alessandro, J. L. Pellequer, M. Odorico, V. Mattoli and M. Giorgi, *Int. J. Nanomed.*, 2012, **7**, 19–24.
- 76 G. Ciofani, S. Danti, S. Nitti, B. Mazzolai, V. Mattoli and M. Giorgi, *Int. J. Pharm.*, 2013, **444**, 85–88.
- 77 A. Salvetti, L. Rossi, P. Iacopetti, X. Li, S. Nitti, T. Pellegrino, V. Mattoli, D. Golberg and G. Ciofani, *Nanomedicine*, 2015, **10**, 1911–1922.
- 78 M. H. Saier Jr., *Enzymes in Metabolic Pathways. A comparative study of mechanism, structure, evolution and control*, Harper & Row Publishers, New York, 1987, 48–59.
- 79 C. Parra, F. Montero-Silva, R. Henríquez, M. Flores, C. Garín, C. Ramírez, M. Moreno, J. Correa, M. Seeger and P. Häberle, *ACS Appl. Mater. Interfaces*, 2015, **7**, 6430–6464.
- 80 V. R. S. S. Mokkapatil, N. P. Tasli, Z. Khan, A. Tufani, S. Pandit, H. Budak and F. Sahin, *RSC Adv.*, 2016, **6**, 56159–56165.
- 81 S. Liu, T. H. Zeng, M. Hofmann, E. Burcombe, J. Wei, R. Jiang, J. Kong and Y. Chen, *ACS Nano*, 2011, **5**, 6971.
- 82 W. Hu, C. Peng, W. Luo, M. Lv, X. Li, D. Li, Q. Huang and C. Fan, *ACS Nano*, 2010, **4**, 4317–4323.



- 83 O. N. Ruiz, K. A. Fernando, B. Wang, N. A. Brown, P. G. Luo, N. D. McNamara, M. Vangsness, Y. Sun and C. E. Bunker, *ACS Nano*, 2011, **5**, 8100–8107.
- 84 A. M. Pinto, S. Moreira, I. C. Gonçalves, F. M. Gama, A. M. Mendes and F. D. Magalhães, *Colloids Surf., B*, 2013, **104**, 229–238.
- 85 G. Gollavelli and Y. Ling, *Biomaterials*, 2012, **33**, 2532–2545.
- 86 V. K. Rana, M. Choi, J. Kong, G. Y. Kim, M. J. Kim, S. Kim, S. Mishra, R. P. Singh and C.-S. Ha, *Macromol. Mater. Eng.*, 2011, **96**, 131–140.
- 87 I. Lasocka, L. Szulc-Dabrowska, M. Skibniewski, E. Skibniewska, W. Strupinski, I. Pasternak, H. Kmiec and P. Kowalczyk, *Toxicol. In Vitro*, 2018, **48**, 276–285.
- 88 P. Zhang, H. Wang, X. Zhang, W. Xu, Y. Li, Q. Li, G. Wei and Z. Su, *Biomater. Sci.*, 2015, **3**, 852–860.

